Cell Reports
Physical Science

CellPress
OPEN ACCESS

Report

The role of electrons' spin in DNA oxidative damage recognition

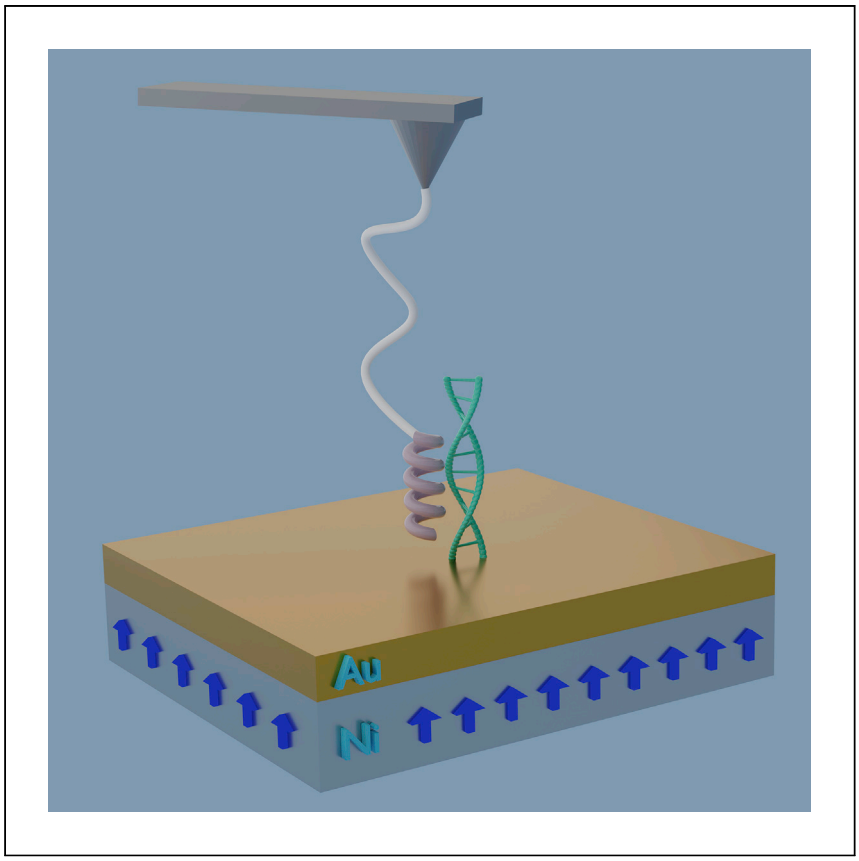

Understanding how DNA damage is found and repaired by enzymes in the cell is of high importance. Zhu et al. propose that the enzyme-DNA recognition process involves charge and electrons' spin polarization, revealing a possible mechanism for damage detection "from a distance.".

Qirong Zhu, Yael Kapon, Aaron M. Fleming, ..., Cynthia J. Burrows, Yossi Paltiel, Ron Naaman

burrows@chem.utah.edu (C.J.B.)
paltiel@mail.huji.ac.il (Y.P.)
ron.naaman@weizmann.ac.il (R.N.)

Highlights

DNA is oxidatively damaged at different locations

The enzyme-DNA recognition process involves charge and electrons' spin polarization

The importance of the electrons' spin in bio-related interactions in general

Zhu et al., Cell Reports Physical Science 3, 101157
December 21, 2022
https://doi.org/10.1016/j.xcrp.2022.101157

Cell Reports
Physical Science

CellPress
OPEN ACCESS

Report

The role of electrons' spin in DNA oxidative damage recognition

Qirong Zhu,[1,6] Yael Kapon,[2,6] Aaron M. Fleming,[3] Suryakant Mishra,[1] Kakali Santra,[1] Francesco Tassinari,[1,4] Sidney R. Cohen,[5] Tapan Kumar Das,[1] Yutao Sang,[1] Deb K. Bhowmick,[1] Cynthia J. Burrows,[3,*] Yossi Paltiel,[2,*] and Ron Naaman[1,7,*]

SUMMARY

Formation of 8-oxo-7,8-dihydro-2′-deoxyguanosine (OG) is one of the most common forms of DNA oxidative damage found in human cells. Although this damage is prevalent in many disease states, it only marginally influences the structure and stability of double-stranded DNA (dsDNA). Therefore, it is a challenge to establish the mechanism by which this damage is detected by repair enzymes. We investigated the position-dependent effect of the damage on the interactions between dsDNA and oligopeptides using atomic force microscopy. The results were confirmed by monitoring the spin and location-dependent polarizability of the damaged DNA, applying a Hall device. The observations suggest that the interaction of peptide with DNA depends on oxidative damage in the DNA and on its location relative to the point of contact between the peptide and the DNA. Hence, a remote search mechanism for damage in DNA is possible.

INTRODUCTION

The sequence of bases in the DNA molecule carries specific genetic information: its consistency throughout the life of the organism plays a critical role in transcription and replication processes.[1] However, intact DNA is subject to damage, including base-pair mismatches and oxidation.[2] Accordingly, cellular mechanisms continuously repair the DNA structure to avoid mutagenesis. Understanding how DNA damage is found and repaired by enzymes in the cell is therefore of high importance.[3] Despite extensive work, many features of the search process are still unknown, for example, it is not understood how the repair enzyme recognizes the damage and from what distance.[4–7] The present study aims at revealing a possible mechanism for damage detection "from a distance." We propose that the enzyme-DNA recognition process involves charge and spin polarization. This hypothesis was tested by using two complementary techniques. In the first, we investigated spin-dependent polarization of the DNA samples by Hall-effect measurements.[8] The second method was atomic force microscope-based single-molecule force spectroscopy (AFM-SMFS), which is relatively popular due to its simple sample preparation requirements and applicability under near-physiological conditions.[9] This technique measures the mean pulling force (MPF), which is used to probe the affinity, mechanics, and recognition properties of interactions between pairs of biomolecules such as antibody/antigen,[10] ligand/receptor pairs,[11,12] protein/DNA,[13] or DNA/DNA.[14]

Following initial studies of the interaction between two fully matched single strands of DNA,[15–17] efforts became focused on harnessing DNA as a tool for molecular

[1]Department of Chemical and Biological Physics, Weizmann Institute of Science, Rehovot 76100, Israel

[2]Department of Applied Physics, Center for Nano-Science and Nano-Technology, The Hebrew University of Jerusalem, Jerusalem 9190401, Israel

[3]Department of Chemistry, University of Utah, 315 South 1400 East, Salt Lake City, UT 84112-0850, USA

[4]Department of Chemical and Geological Sciences, University of Modena and Reggio Emilia, 41125 Modena, Italy

[5]Department of Chemical Research Support, Weizmann Institute of Science, Rehovot 76100, Israel

[6]These authors contributed equally

[7]Lead contact

*Correspondence:
burrows@chem.utah.edu (C.J.B.),
paltiel@mail.huji.ac.il (Y.P.),
ron.naaman@weizmann.ac.il (R.N.)

https://doi.org/10.1016/j.xcrp.2022.101157

recognition of proteins and peptides.[18–22] Only a few studies attempted to identify mismatch damage within the DNA itself. It was shown that mismatched DNA can be distinguished by the discrepancy of base stacking.[23] Furthermore, an addressable DNA origami scaffold allowed precise detection of a statistically significant difference of 4 pN in the rupture force per each additional mismatched base-pair.[24] However, DNA with oxidative damage has not been studied until now because the damage does not modify the base stacking structure and is thus a challenge for AFM-SMFS.

In this work, we show that the interaction between oligopeptide and damaged DNA can be sensed by AFM-SMFS that is also sensitive to the electrons' spin-dependent force, by combining it with the chiral-induced spin selectivity (CISS) effect.[25]

According to the CISS effect, charge reorganization in chiral systems depends on the electron spin. Namely, electrons with their spin aligned parallel to their velocity will move at different speeds compared with electrons with their spin aligned antiparallel to the velocity. The handedness of the molecule controls which spin direction will enhance the electron flow.[26] Here a chiral oligopeptide is attached to the AFM tip and allowed to interact with surface bound monolayers of double-stranded DNA (dsDNA) having guanine or adenine oxidative base damage (OG or 8-oxo-7,8-dihydro-2′-deoxyadenosine [OA], respectively) localized in different positions along the molecular chain: proximal (close to substrate), distal (close to exposed end of molecule), or central. The measurements were performed in a physiological solution. The oligopeptide chosen for attachment at the end of the AFM tip mimics an enzyme approaching the damaged DNA.

RESULTS

Hall Effect-based measurement on damaged dsDNA

To understand how the position of the oxidative damage affects the potential for spin, we studied the spin-dependent polarization using Hall Effect-based devices (see Figure 1).[8,27] This device probes the surface magnetization that is induced by the damaged DNA. The four probes of a Hall device were prepared from a GaN/AlGaN wafer having a two-dimensional electron gas (2DEG) layer as a conducting channel. The conducting channel is coated with a 5 nm gold film upon which a monolayer of the dsDNA was bound covalently through a gold-sulfur bond. Figure 1A shows a schematic diagram of the setup. The details of the fabrication of these devices and the operational mode are reported elsewhere.[8,28] An electric potential applied between the gate and the Hall device charge polarizes the molecules. As a result, charge (either electrons or holes) is injected into the substrate. If this charge injection is spin polarized, it results in a magnetic field, sensed by the Hall device and recorded as a small voltage. Sequential gate voltages from −50 V to 50 V in steps of 10 V were applied. Figure 1B shows the representative Hall potential obtained from each dsDNA sample, i.e., distal, central, and proximal OG, as a function of the applied gate voltage. A sharp peak appears at each step in the gate voltage and then decays quickly due to the formation of a double layer in the phosphate-buffered saline (PBS solution). Figure 1C presents the Hall potential plotted as a function of gate voltage for the four devices coated with dsDNA containing OG at the three different locations as well as the fully matched DNA (see the materials section of the supplemental information). The Hall potential depends linearly on the applied voltage between the gate and the device. The relative slopes obtained for distal OG, central OG, proximal OG, and the fully matched DNA are 1.0: 0.2: 0.5: 0.2, respectively. Interestingly, a fully matched DNA and a DNA with unmatched bases

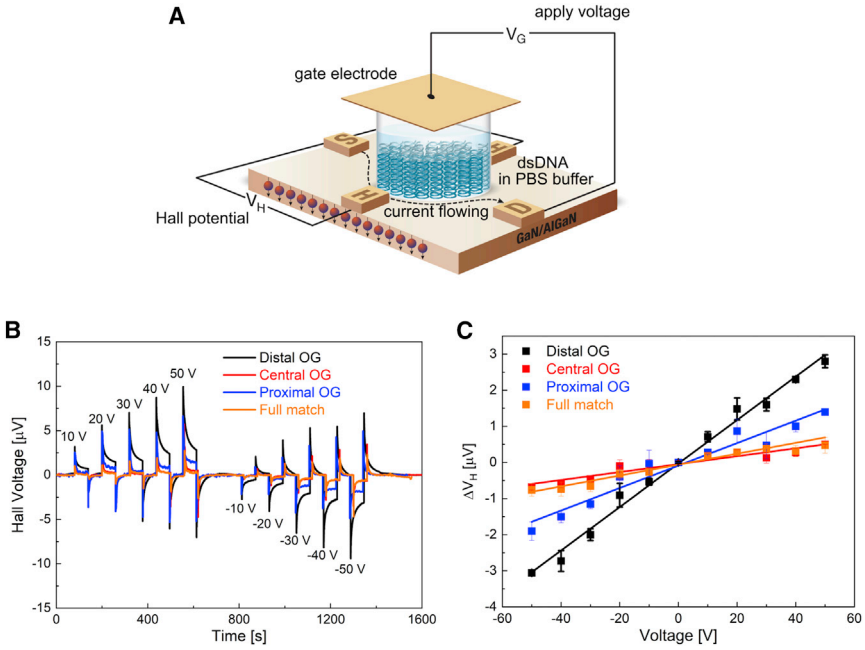

Figure 1. Spin-dependent polarization of dsDNA with guanine oxidative damage

(A) Schematic diagram of the Hall-effect setup for spin-dependent polarization measurements. Gate voltages from −50 V to +50 V were applied in steps of 10 V between a gate electrode and a Hall device coated with a dsDNA monolayer.

(B) Representative Hall potentials were obtained on distal OG, central OG, proximal OG, and fully matched dsDNA monolayers, with sequential gate pulses from −50 V to +50 V.

(C) Hall voltage measured from four different devices as a function of the gate voltage. Error bars represent the standard error.

show similar results. (see Figure S1). It is clear that different spin accumulation is measured on the gold surface attached to the DNA depending on the OG defect location. A larger effect is measured if the defect is at one of the ends of the DNA. We address this phenomenon following presentation of the results from the AFM-SMFS complementary experiment.

Force spectroscopy between oligopeptide and damaged DNA

When a chiral oligopeptide-modified AFM tip approaches the DNA molecules adsorbed on a ferromagnetic substrate, charge redistribution occurs in the DNA. The MPF depends on the electrical dipole-dipole interactions and spin-exchange interactions. Both depend on the amount of charge and its spin polarization accumulated at the contact point between the oligopeptide adsorbed on the AFM tip and the DNA adsorbed on the ferromagnetic substrate (See Figure 2).[25,29] The amount of charge that can penetrate from the ferromagnetic substrate into the DNA depends on the magnetization of the substrate, which defines the spin orientation of the ejected electrons.[30] The dsDNA was adsorbed on the magnetic surface with proximal, central, or distally positioned OG or OA. Hence, the AFM-SMFS experiments probed the effect of the damage and its position on the ability of charge and spin to accumulate at the contact point between the oligopeptide and the DNA.

A previous work examined enantiospecific interactions between chiral molecules and a ferromagnetic surface governed by the exchange interactions using modified AFM-SMFS.[29] Another study used this method to examine enantiospecific interactions between chiral molecules.[25] A similar method (schematically shown in Figure 3A) is

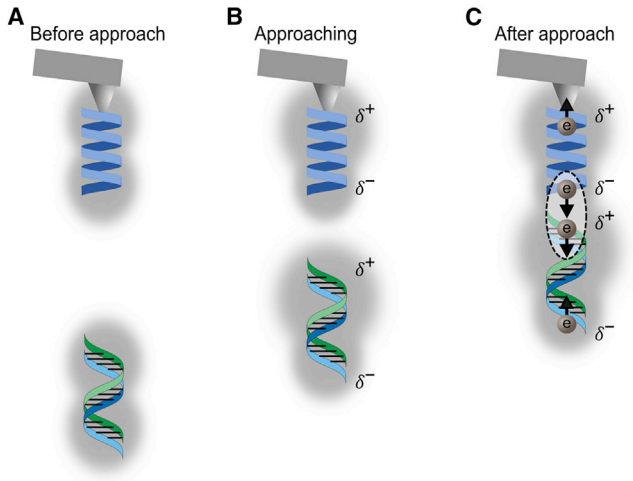

Figure 2. A scheme describing the interaction between the oligopeptide attached to the AFM tip and the dsDNA

(A) Large distance between the AFM tip and the DNA.

(B) As the AFM tip approaches the DNA, the charge is redistributed so that an induced-dipole induced-dipole long-range interaction exists.

(C) At contact, the charge redistribution is accompanied by spin polarization and in addition to the dipole-dipole interaction also a spin-exchange interaction takes place.

applied here to examine short-ranged spin-exchange interactions between a helical molecule on the AFM tip (L-36-alpha helix polyalanine, abbreviated as L-AHPA) and dsDNA containing oxidative damage in different locations. The DNA molecules are adsorbed on a substrate consisting of a gold-coated nickel film on silicon (Ni/Au: 120 nm/8 nm). The AFM tip approached the surface and then pulled away, while recording the force required to detach the tip from the surface. Sharp tips were used to enhance the localization of the exchange interaction measurements. A magnet directly attached to the back of the ferromagnetic nickel/gold substrate provided a magnetic field perpendicular to the sample surface with either north or south pole pointing up (up or down magnetization). The role of the magnetic field is to spin-polarize the nickel layer on the substrate. Experiments were performed in PBS solution. The specific sequences used are shown in the supplemental information.

Former studies established that the mechanical properties of biological systems depend in a nonlinear fashion on the loading rate at which they are measured.[31] The loading rate is associated with the unbinding energy of the probed molecule. There are three methods to control the unloading rate: pulling the cantilever at different speeds, using cantilevers with different spring constants, or controlling the force rather than the rate. In pulling events, the mechanics of DNA overstretching (irreversible stretching) is sequence-dependent.[32] All the DNA strands used in this work have the same sequence with only the position of the OG or OA shifted. Therefore, it is reasonable to assume that in this study the overstretching was the same for all samples. To reduce random error, the same cantilever and conditions were used for each sample while measuring with up and down magnetization.[21] To minimize the influence from free DNAs or peptides, we washed the samples with the PBS buffer between measurements at different direction of the magnetic field.[22]

The chiral oligopeptide is connected to the tip through a 40-nm-long polyethylene glycol (PEG) that acts as a spacer between the tip and the oligopeptide-DNA interaction. This allows one to differentiate between specific interaction between the

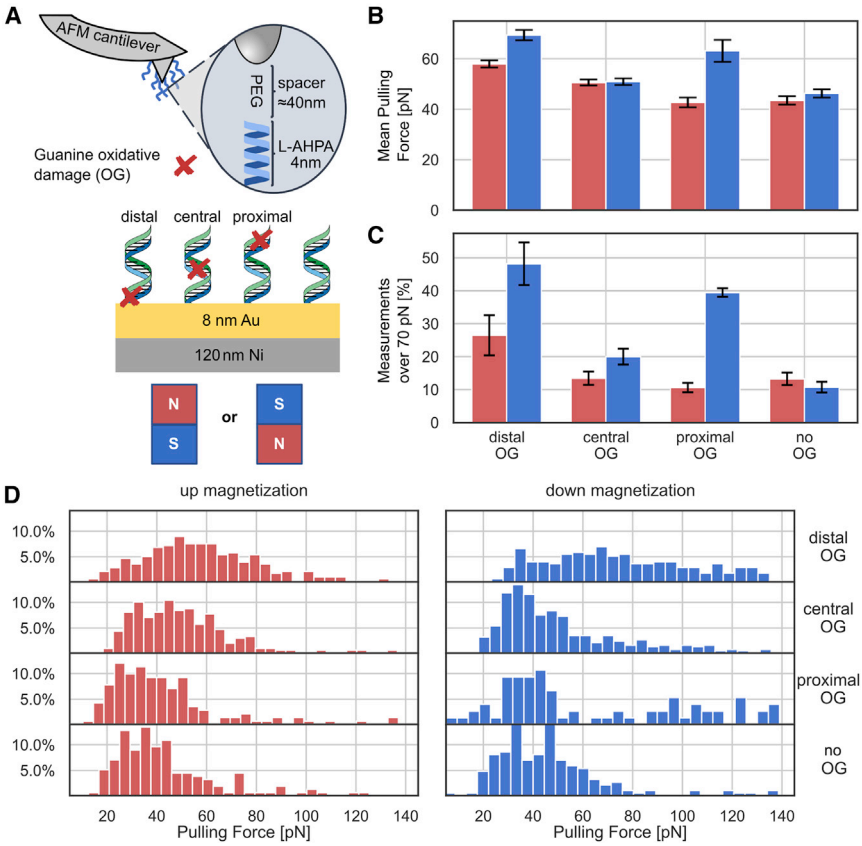

Figure 3. SMFS measurements of dsDNA with different locations of guanine oxidative damage

(A) A schematic diagram of the AFM-SMFS measurements. A flexible PEG linker with a length of 40 nm was bound to a sharp Si3N4 tip and then connected to a helical molecule (L-AHPA) with a length of 4 nm. The dsDNA monolayer is adsorbed on Ni (120 nm)/Au (8 nm) substrate magnetized either up (red) or down (blue). The experiment was performed in PBS buffer (pH = 7.2).

(B) Mean pulling force between the helical molecule on the tip (L-AHPA) and different dsDNA monolayers (described in the text). Error bars represent the standard error.

(C) Statistics for pulling force events above 70 pN represented as a percentage of the total number of measurements. The error bars are calculated as the change in counts for 3 pN shift in the cutoff.

(D) Histograms of the pulling force between the helical molecule on the tip (L-AHPA) and dsDNA monolayers. The pulling force was recorded at a retracting speed of 200 nm s^{-1}.

molecules and nonspecific interaction with the tip. Due to the PEG molecule size, we expect only one to two molecules to be on the tip and interact with the substrate each time. In addition, any small variations in the number of molecules interacting are averaged out in the large statistics.

Over a thousand force versus distance curves were measured and subsequently examined manually. Only curves that showed a clear pulling off feature were further considered as single-molecule rupture events (Figure S2). A worm-like chain (WLC) model[33] was then fitted to the specific interaction pulling event and the pulling force was retrieved. Figure 3D summarizes the resultant pulling forces between the helical molecule and dsDNA monolayers under up and down magnetization. The MPF was calculated as the mean of all pulling events deemed to be valid. Figure 3B presents the MPF for each OG position in both magnetic field directions. In the case of distal OG, the MPF values for up and down magnetization are 58 $\pm$ 1 pN and 69 $\pm$ 2 pN, respectively. For central OG, the MPF values under up and down magnetization are

both 51 ± 1 pN. Proximal OG shows a much higher MPF for the down magnetization (63 ± 4 pN) than for up magnetization (43 ± 2 pN). As a control experiment, the same measurements were performed on a dsDNA with no OG but with two adenine-cytosine (AC) mismatches located at the same positions and gave values under up and down magnetization of 44 ± 2 pN and 46 ± 2 pN, respectively. For reference, in a fully matched dsDNA sample with no OG and no mismatches, a force of about 60 pN was measured for both magnetizations (Figure S3). This suggests that the pull-off force value is sensitive to distortion of the DNA base-pair structure by mismatch, an effect independent of the magnetization direction. The dependence of the force on the direction of magnetization is a clear indication for the role of spin-polarized electrons in the interaction between the oligopeptide on the tip and the adsorbed DNA.[30]

To emphasize the role of the spin interaction on the MPF, we differentiated between the high, spin-originated force, and the low electrostatic forces. Figure 3C presents the fraction of measurements in which the force exceeds 70 pN, which is the maximal force that it can be stretched without leading to distortion of the overall structure.[32,34] The direction of magnetization has a larger effect when the pulling force is above 70 pN. The surprise finding here is that while damage at the distal and proximal positions shows similar forces and similar dependence on magnetization direction, both the force and the dependence on the magnetization are reduced significantly for the oxidative damage at the center of the DNA. This is consistent with the Hall measurements presented above. For the unfavored magnetization, there is a steady decline of the force from distal to middle to proximal positions in the strand.

To show that the behavior for OG is general for oxidative damage, the AFM-SMFS and some Hall measurements were performed for dsDNA with OA as the oxidative damage (Figures S4 and S5). Although the overall forces between the tip's peptide and the DNA strands with OA are much weaker, the same trends as in the case of OG are observed. For both distal OA and central OA, no significant dependence of the force on the magnetization direction can be observed. Most notably, the biggest difference in MPF between up and down magnetization is in the proximal OA, as was observed with the OG case. Distal and proximal OA both presented a much weaker Hall potential than for OG. This is consistent with OG having a significant effect on the spin transport through the molecule.[28] The results obtained with OA, although not as dramatic as those obtained with OG, still indicate a similar effect of the damage on the interaction of DNA with the oligopeptide.

DISCUSSION

The dependence of the MPF on the direction of magnetization of the substrate (Figure 3) indicates that upon approach of the tip to the DNA monolayer, charge is injected from the substrate to the adsorbed molecules. Because the molecules are chiral and due to the CISS effect, the efficiency of charge injection depends on the spin of the injected charge, which in turn depends on the direction of the magnetization of the substrate. Hence, the spin direction affects the efficiency of charge injection from the substrate and the MPF measurements probe the amount of charge and spin in contact with the oligopeptide attached to the tip, through dipole-dipole interactions. These observations are consistent with the spin polarization measured with the Hall device (Figure 1).

Previous studies on DNA with OG found that the OG tends to increase the spin selectivity for electrons moving through the DNA. Namely, it serves as a higher barrier for

transport, so that it reduces the total charge polarization, but enhances the relative conductivity of the preferred spin through the damaged region, thus improving the spin selectivity.[28,35] Hence, the force (F) measured is given by $F \propto CP + B$, where C is the charge polarization and P is the spin polarization, and B represents other forces that do not depend on the spin. Interestingly the Hall signal is also proportional to CP and indeed the results obtained by the two measuring methods are correlated. The charge polarization depends on the length of the undamaged part of the DNA. While the DNA with the central OG has the lowest charge polarization, the undamaged DNA has the lowest spin polarization. Therefore, those two samples show the smallest force and negligible effect of the spin, as indicated by the small difference in the force for the magnetic field pointing up or down.

It is interesting to note that in the case of a DNA duplex containing mismatched bases that was investigated as a reference, no effect of the direction of spin injected from the substrate on the force was observed and in general, the force measured was smaller than for DNA with OG. This can be explained by lower polarizability due to diminished conduction of electrons through the dsDNA as result of the damage.[28]

In conclusion, our experiments indicate that charge and spin polarization may play an important role in affecting the interaction between enzymes and DNA and serve as markers for the location of oxidative damage. The OG results in the enhancement of spin polarization in the DNA. The MPF of distal OG, central OG, and proximal OG in dsDNA in the preferred spin direction (down magnetization) is consistent with spin-dependent polarization measured by the Hall-based setup. Differing MPF for the two magnetization directions is only observed when oxidative damage is present and relates to the length of the chiral structure. Overall, CISS-based interactions enhance the sensitivity of AFM-SMSF, enabling the detection and localization of OG. Measurements on dsDNA with OA suggest that these conclusions can be extended to other defects in DNA. It is important to appreciate that *in vivo*, upon the approach of a protein to the DNA, charge reorganization is induced in the DNA. Since the DNA is chiral, the charge moving in the DNA is spin polarized.[36,37] In this case, the entire DNA molecule can contribute spin-polarized charge to the point of interaction, in the same way the ferromagnetic substrate acts in the present study. This work suggests that the interaction between a repair enzyme and damaged DNA is sensitive to long-range affects and may depend on the effective charge and spin polarization that provide information on the location of the damage.

EXPERIMENTAL PROCEDURES

Resource availability

Lead contact

Further information and requests for resources and reagents should be directed to and will be fulfilled by the Lead Contact, Ron Naaman (ron.naaman@weizmann.ac.il).

Materials availability

This study did not generate new unique materials.

Data and code availability

Force curve data during this study will be shared by the lead contact upon request. No original code is reported in this work.

Materials

(3-Aminopropyl)trimethoxysilane (APTMS) was purchased from Sigma-Aldrich. Maleimide-poly(ethylene glycol)-succinimidyl carboxyl methyl ester (MAL-PEG-SCM,

5k) was purchase from Creative PEGworks. L (form) HS-CH_2CH_2-CO-NH-$(AAAAK)_7$-COOH) (L-AHPA) was purchased from hylabs. The silicon nitride (Si_3N_4) AFM tips used in this work were SNL-10 (cantilever D, nominal tip radius = 2 nm, nominal spring constant = 0.06 N/m). The single-stranded DNA oligomers without oxidative damage were purchased from Syntezza.

Molecule synthesis

The oxidatively damaged DNA oligomers were synthesized and deprotected by the DNA/Peptide core facility at the University of Utah following standard protocols. The site-specific introduction of the 8-oxo-7,8-dihydro-2′-deoxyguanosine was achieved using a commercially available phosphoramidite (Glen Research). The crude oligomers were purified using an anion-exchange HPLC column running a mobile phase system consisting of A (1 M sodium chloride, 20 mM sodium phosphate at pH 7 in 1:9 MeCN:ddH_2O water) and B (1:9 MeCN:ddH_2O). The method was initiated at 20% B and increased to 100% B via a linear gradient over 30 min with a flow rate of 1 mL/min while monitoring the absorbance at 260 nm. The purified samples were dialyzed in ddH_2O for 36 h to remove the purification salts, and then lyophilized to dryness and resuspended in ddH_2O. The sample concentrations were determined from the absorbance at 260 nm, using the nearest neighbor approximation while substituting G for OG to obtain the extinction coefficient for calculating the concentrations of the purified stock DNA oligomer samples.

Surface and tip modification

The silicon nitride AFM tip with a nominal radius of 2 nm was first cleaned by piranha solution (3 parts of 95%–98% sulfuric acid and 1 part of 30% hydrogen peroxide solution) for 10 min, followed by rinsing in boiling high pure water twice and then cleaned by a UV-ozone treatment for 15 min in a humid environment. The cleaned tip was dried in a gentle nitrogen steam and then immersed into APTMS/toluene (volume ratio: 1:9) for 24 h. After this, the tip was sequentially rinsed with toluene, toluene/acetone (volume ratio: 1:1), and acetone. After rinsing the tip, it was immersed in 50 mM BB buffer (pH = 8.5) for 1 h and then immersed in MAL-PEG-SCM for 1 h.[38] The PEG modified tip was rinsed by high pure water and then immersed in L-AHPA mixed with 1–2 mM TECP in 0.1 M PBS buffer at 4°C for 12 h. Finally, the modified tip was rinsed in 0.1 M PBS and kept in 0.1 M PBS at 4°C before using (Figures S6–S8). The dsDNA monolayer is bound to a silicon substrate covered with a gold-coated nickel film (Ni/Au: 120 nm/8 nm). This substrate was first cleaned by immersing in boiling acetone and ethanol for 10 min, then treated by a UV-ozone cleaning for 15 min and finally incubated in warm ethanol for 40 min then dried by nitrogen before incubation with dsDNA. The dsDNA solution was formed by two complementary single-stranded DNAs by using PCR thermal incubation (90°C for 10 min, then cooled down to 15°C at the rate of −1°C per 2 min). The dsDNA solution was mixed with Tris(2-carboxyethyl)phosphine hydrochloride (TCEP) in 0.4 M PBS buffer (pH = 7.2). The solution was left in 5 mM tris buffer for 2 h and then filtered by a Micro Bio-Spin P-30 column. The solution was then immediately dropcast onto a dried Ni/Au substrate and incubated for 20 to 24 h in a humid environment. After incubation, the sample was rinsed by 0.4 M PBS and then deionized water (Figures S9 and S10).

DNA characterization

The DNA with well-defined and characterized damage was prepared and analyzed following the procedure described by Zhou et al.[39] The presence of a band at 1655 cm^{-1} measured by polarization modulation-infrared reflection-adsorption spectroscopy (PM-IRRAS) demonstrates the existence of dsDNA on the gold substrate, while it is absent in the single-stranded DNA. This has been shown in Figure S10 and in

reference given therein. All the monolayers were characterized also by XPS and no significant difference between thicknesses/coverage was found (see Table S1).

AFM-based SMFS

The force spectroscopy function of a Nanowizard 3 (JPK) was applied for the measurements. The tip was approached to the surface at 1 μm/s and retracted at 0.2 μm/s. After completing the measurements on the dsDNA samples, the photodiode sensitivity was calibrated from the slope of deflection versus distance curve of the functionalized AFM tip on the bare Ni (120 nm)/Au (8 nm) covered silicon substrate.[40] This sensitivity value, combined with thermal tune of the cantilever in the JPK software to deduce the spring constant, were used for calculating force values. Over 1,000 force versus distance curves were taken. Only the curves that showed a significant pulling event were then analyzed by the JPK data analysis software. The WLC model was fitted to the pulling events to find the rupture point and pulling force (Figure S1). The MPF was retrieved by averaging the pulling forces. The applied magnetic field was 0.3 T.

Hall measurement

A dual-channel Keithley 2636A source unit was used to generate the current between the source (S) and the drain (D) electrodes and to apply gate voltages between the gate electrode and the Hall device. The Hall voltage (V_H) was obtained by a Keithley 2182A nanovoltmeter. Current was set to follow through both the forward and backward directions to calibrate the Hall voltage attributed to its asymmetry of Hall devices. The Hall potential was defined by the formula, $\Delta V_H = V_{H+} - V_{H-}$. All measurements were performed in 0.1 M PBS buffer.[28]

SUPPLEMENTAL INFORMATION

Supplemental information can be found online at https://doi.org/10.1016/j.xcrp.2022.101157.

ACKNOWLEDGMENTS

The authors acknowledge the support from Dr. Tatyana Bendikov and Dr. Yifeng Cao. R.N. acknowledges the support of the Israel Science Foundation and of the Air Force Office of Scientific Research Grant FA9550-21-1-0418. C.J.B. thanks the U.S. National Science Foundation (CHE-1808475) for supporting this work.

AUTHOR CONTRIBUTIONS

A.F. synthesized dsDNA with oxidative damage. Q.R.Z. performed the AFM tip modification with support from Y.T. and D.K.B. Q.R.Z. performed single-molecule force spectroscopy experiments with guidance from S.C. Y.K. and Q.R.Z. analyzed the force data. S.M., Q.R.Z., K.S., and F.T. performed Hall device measurements. S.M. and T.K.D. fabricated the Hall chips. Q.R.Z., Y.K., S.C., F.T., A.F., and R.N. wrote the manuscript. R.N., Y.P., and C.J.B. conceived the experiments and guided the project.

DECLARATION OF INTERESTS

The authors declare no competing interests.

Received: September 14, 2022
Revised: October 15, 2022
Accepted: October 27, 2022
Published: November 28, 2022

REFERENCES

1. Aggarwal, A., Naskar, S., Sahoo, A.K., Mogurampelly, S., Garai, A., and Maiti, P.K. (2020). What do we know about DNA mechanics so far? Curr. Opin. Struct. Biol. *64*, 42–50. https://doi.org/10.1016/j.sbi.2020.05.010.

2. Yousefzadeh, M., Henpita, C., Vyas, R., Soto-Palma, C., Robbins, P., and Niedernhofer, L. (2021). DNA damage—how and why we age? Elife *10*, e62852. https://doi.org/10.7554/eLife.62852.

3. Jackson, S.P., and Bartek, J. (2009). The DNA-damage response in human biology and disease. Nature *461*, 1071–1078. https://doi.org/10.1038/nature08467.

4. Clancy, S. (2008). DNA damage & repair: mechanisms for maintaining DNA integrity. Nature Education. https://www.nature.com/scitable/topicpage/dna-damage-repair-mechanisms-for-maintaining-dna-344/.

5. Cadet, J., and Davies, K.J.A. (2017). Oxidative DNA damage & repair: an intro-duction. Free Radic. Biol. Med. *107*, 2–12. https://doi.org/10.1016/j.freeradbiomed.2017.03.030.

6. Schaich, M.A., and Van Houten, B. (2021). Searching for DNA damage: in-sights from single molecule analysis. Front. Mol. Biosci. *8*, 772877. https://doi.org/10.3389/fmolb.2021.772877.

7. Yavin, E., Stemp, E.D.A., O'shea, V.L., David, S.S., and Barton, J.K. (2006). Electron trap for DNA-bound repair enzymes: a strategy for DNA-mediated signaling. Proc. Natl. Acad. Sci. USA *103*, 3610–3614. https://doi.org/10.1073/pnas.060023910.

8. Kumar, A., Capua, E., Vankayala, K., Fontanesi, C., and Naaman, R. (2017). Magnetless device for conducting three-dimensional spin-specific electrochemistry. Angew Chem. Int. Ed. Engl. *56*, 14587–14590. https://doi.org/10.1002/anie.201708829.

9. Neuman, K.C., and Nagy, A. (2008). Single-molecule force spectroscopy: optical tweezers, magnetic tweezers and atomic force microscopy. Nat. Methods *5*, 491–505. https://doi.org/10.1038/nmeth.1218.

10. Liu, H., Schittny, V., and Nash, M.A. (2019). Removal of a conserved disulfide bond does not compromise mechanical stability of a VHH anti-body complex. Nano Lett. *19*, 5524–5529. https://doi.org/10.1021/acs.nanolett.9b02062.

11. Florin, E.L., Moy, V.T., and Gaub, H.E. (1994). Adhesion forces between individual ligand-receptor pairs. Science *264*, 415–417. https://doi.org/10.1126/science.8153628.

12. Baumann, F., Bauer, M.S., Milles, L.F., Alexandrovich, A., Gaub, H.E., and Pippig, D.A. (2016). Monovalent Strep-Tactin for strong and site-specific tethering in nanospectroscopy. Nat. Nanotechnol. *11*, 89–94. https://doi.org/10.1038/nnano.2015.231.

13. Ritzefeld, M., Walhorn, V., Anselmetti, D., and Sewald, N. (2013). Analysis of DNA interactions using single-molecule force spectroscopy. Amino Acids *44*, 1457–1475. https://doi.org/10.1007/s00726-013-1474-4.

14. Strunz, T., Oroszlan, K., Schäfer, R., and Güntherodt, H.J. (1999). Dynamic force spectroscopy of single DNA molecules. Proc. Natl. Acad. Sci. USA *96*, 11277–11282. https://doi.org/10.1073/pnas.96.20.11277.

15. Lee, G.U., Chrisey, L.A., and Colton, R.J. (1994). Direct measurement of the forces between complementary strands of DNA. Science *266*, 771–773. https://doi.org/10.1126/science.7973628.

16. Clausen-Schaumann, H., Rief, M., Tolksdorf, C., and Gaub, H.E. (2000). Mechanical stability of single DNA molecules. Biophys. J. *78*, 1997–2007. https://doi.org/10.1016/S0006-3495(00)76747-6.

17. Fisher, T.E., Marszalek, P.E., and Fernandez, J.M. (2000). Stretching single molecules into novel conformations using the atomic force micro-scope. Nat. Struct. Biol. *7*, 719–724. https://doi.org/10.1038/78936.

18. Bartels, F.W., McIntosh, M., Fuhrmann, A., Metzendorf, C., Plattner, P., Sewald, N., Anselmetti, D., Ros, R., and Becker, A. (2007). Effector-stimulated single molecule protein-DNA interactions of a quorum-sensing system in sinorhizobium meliloti. Biophys. J. *92*, 4391–4400. https://doi.org/10.1529/biophysj.106.082016.

19. Chung, J.W., Shin, D., Kwak, J.M., and Seog, J. (2013). Direct force measure-ment of single DNA-peptide interactions using atomic force microscopy. J. Mol. Recogn. *26*, 268–275. https://doi.org/10.1002/jmr.2269.

20. Wollschläger, K., Gaus, K., Körnig, A., Eckel, R., Wilking, S.D., McIntosh, M., Majer, Z., Becker, A., Ros, R., Anselmetti, D., and Sewald, N. (2009). Single-molecule experiments to elucidate the minimal requirement for DNA recognition by transcription factor epitopes. Small *5*, 484–495. https://doi.org/10.1002/smll.200800945.

21. Eckel, R., Ros, R., Ros, A., Wilking, S.D., Sewald, N., and Anselmetti, D. (2003). Identification of binding mechanisms in single molecule–DNA complexes. Biophys. J. *85*, 1968–1973. 1968–1973. https://doi.org/10.1016/S0006-3495(03)74624-4.

22. Eckel, R., Wilking, S.D., Becker, A., Sewald, N., Ros, R., and Anselmetti, D. (2005). Single-molecule experiments in synthetic biology: an approach to the affinity ranking of DNA-binding peptides. Angew Chem. Int. Ed. Engl. *44*, 3921–3924. https://doi.org/10.1002/anie.200500152.

23. Sattin, B.D., Pelling, A.E., and Goh, M.C. (2004). DNA base pair resolution by single molecule force spectroscopy. Nucleic Acids Res. *32*, 4876–4883. https://doi.org/10.1093/nar/gkh826.

24. Liu, W., Guo, Y., Wang, K., Zhou, X., Wang, Y., Lü, J., Shao, Z., Hu, J., Czajkowsky, D.M., and Li, B. (2019). Atomic force microscopy-based single-molecule force spectroscopy detects DNA base mismatches. Nanoscale *11*, 17206–17210. https://doi.org/10.1039/C9NR05234H.

25. Kapon, Y., Saha, A., Duanis-Assaf, T., Stuyver, T., Ziv, A., Metzger, T., Yochelis, S., Shaik, S., Naaman, R., Reches, M., and Paltiel, Y. (2021). Evidence for new enantiospecific interaction force in chiral biomolecules. Chem *7*, 2787–2799. https://doi.org/10.1016/j.chempr.2021.08.002.

26. Naaman, R., Paltiel, Y., and Waldeck, D.H. (2020). Chiral molecules and the spin selectivity effect. J. Phys. Chem. Lett. *11*, 3660–3666. https://doi.org/10.1021/acs.jpclett.0c00474.

27. Eckshtain-Levi, M., Capua, E., Refaely-Abramson, S., Sarkar, S., Gavrilov, Y., Mathew, S.P., Paltiel, Y., Levy, Y., Kronik, L., and Naaman, R. (2016). Cold denaturation induces inversion of dipole and spin transfer in chiral peptide monolayers. Nat. Commun. *7*, 10744. https://doi.org/10.1038/ncomms10744.

28. Mishra, S., Poonia, V.S., Fontanesi, C., Naaman, R., Fleming, A.M., and Burrows, C.J. (2019). Effect of oxidative damage on charge and spin transport in DNA. J. Am. Chem. Soc. *141*, 123–126. https://doi.org/10.1021/jacs.8b12014.

29. Ziv, A., Saha, A., Alpern, H., Sukenik, N., Baczewski, L.T., Yochelis, S., Reches, M., and Paltiel, Y. (2019). AFM-based spin-exchange microscopy using chiral molecules. Adv. Mater. *31*, 1904206. https://doi.org/10.1002/adma.201904206.

30. Ghosh, S., Mishra, S., Avigad, E., Bloom, B.P., Baczewski, L.T., Yochelis, S., Paltiel, Y., Naaman, R., and Waldeck, D.H. (2020). Effect of chiral molecules on the electron's spin wavefunction at interfaces. J. Phys. Chem. Lett. *11*, 1550–1557. https://doi.org/10.1021/acs.jpclett.9b03487.

31. Krieg, M., Fläschner, G., Alsteens, D., Gaub, B.M., Roos, W.H., Wuite, G.J.L., Gaub, H.E., Gerber, C., Dufrêne, Y.F., and Müller, D.J. (2019). Atomic force microscopy-based mechanobiology. Nat. Rev. Phys. *1*, 41–57. https://doi.org/10.1038/s42254-018-0001-7.

32. Rief, M., Clausen-Schaumann, H., and Gaub, H.E. (1999). Sequence-dependent mechanics of single DNA molecules. Nat. Struct. Biol. *6*, 346–349. https://doi.org/10.1038/7582.

33. Milstein, J.N., and Meiners, J.C. (2013). Worm-like chain (WLC). In Encyclopedia of Biophysics, G.C.K. Roberts, ed. (Springer), pp. 2757–2760. https://doi.org/10.1007/978-3-642-16712-6_502.

34. Morfill, J., Kühner, F., Blank, K., Lugmaier, R.A., Sedlmair, J., and Gaub, H.E. (2007). B-S transition in short oligonucleotides. Biophys. J. *93*, 2400–2409. https://doi.org/10.1529/biophysj.107.106112.

35. Mishra, S., Mondal, A.K., Pal, S., Das, T.K., Smolinsky, E.Z.B., Siligardi, G., and Naaman, R. (2020). Length-dependent electron spin polarization in oligopeptides and DNA. J. Phys. Chem. C *124*, 10776–10782. https://doi.org/10.1021/acs.jpcc.0c02291.

36. Göhler, B., Hamelbeck, V., Markus, T.Z., Kettner, M., Hanne, G.F., Vager, Z., Naaman, R., and Zacharias, H. (2011). Selectivity in electron transmission through self-assembled monolayers of double-stranded DNA. Science *331*, 894–897. https://doi.org/10.1126/science.1199339.

37. Xie, Z., Xie, Z., Markus, T.Z., Cohen, S.R., Vager, Z., Gutierrez, R., and Naaman, R. (2011). Spin specific electron conduction through DNA oligomers. Nano Lett. *11*, 4652–4655. https://doi.org/10.1021/nl2021637.

38. Zimmermann, J.L., Nicolaus, T., Neuert, G., and Blank, K. (2010). Thiol-based, site-specific and covalent immobilization of biomolecules for single-molecule experiments. Nat. Protoc. *5*, 975–985. https://doi.org/10.1038/nprot.2010.49.

39. Zhou, J., Fleming, A.M., Averill, A.M., Burrows, C.J., and Wallace, S.S. (2015). The NEIL glycosylases remove oxidized guanine lesions from telomeric and promoter quadruplex DNA structures. Nucleic Acids Res. *43*, 4039–4054. https://doi.org/10.1093/nar/gkv252.

40. Cumpson, P.J.P.J., Zhdan, P., and Hedley, J. (2004). Calibration of AFM cantilever stiffness: a microfabricated array of reflective springs. Ultramicroscopy *100*, 241–251. https://doi.org/10.1016/j.ultramic.2003.10.005.